



**Faculty of Industrial and Manufacturing Technology and
Engineering**

**THERMOSONIC MICRO-INTERCONNECTIONS:
INTERFACIAL Cu-Al INTERMETALLICS COMPOUND GROWTH
STUDIES BASED ON STRESS MODELLING**

Shariza Binti Sharir

Doctor of Philosophy

2024

**THERMOSONIC MICRO-INTERCONNECTIONS:
INTERFACIAL Cu-AI INTERMETALLICS COMPOUND GROWTH
STUDIES BASED ON STRESS MODELLING**

SHARIZA BINTI SHARIR

**A thesis submitted in fulfilment of the requirements for the degree of
Doctor of Philosophy**



Faculty of Industrial and Manufacturing Technology and Engineering

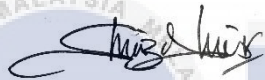
UNIVERSITI TEKNIKAL MALAYSIA MELAKA

2024

DECLARATION

I declare that this thesis entitled “Thermosonic Micro-Interconnections: Interfacial Cu-Al Intermetallics Compound Growth Studies Based On Stress Modelling” is the results of my own research except as cited in the references. The thesis has not been accepted for any degree and is not concurrently submitted in candidature of any other degree.

Signature



Name

Shariza Binti Sharir

Date

18 January 2024



APPROVAL

I hereby declare that I have read this thesis and in my opinion this thesis is sufficient in terms of scope and quality for the award of Doctor of Philosophy.

Signature



:

Supervisor Name

Professor Dr. Mohd Warikh Bin Abdul Rashid

:

Date

18 January 2024

:



DEDICATION

To you, who puts me on top of the world.

and

To all of you, who cared and believed.



“ Success is the sum of small efforts, repeated day in and day out. ”

Robert Collier

*“ The more that you read, the more things you will know,
the more that you learn, the more places you’ll go. ”*

Dr. Seuss

ABSTRACT

One of the most common wire bonding technology involving copper (Cu) wire interconnections is the thermosonic bonding technique. Still, the volumetric changes of intermetallic compounds (IMCs) formed at the bonding interface of Cu wire on Al bond pads induce voids formation in the Cu-Al IMC layer. This is much apparent especially after an annealing treatment of High Temperature Storage (HTS). Effects of Cu free air ball and bonding temperature with high temperature storage (HTS) treatment on Cu-Al bonding interface are unclear due to varying observations and inconsistencies in the bonding parameters. A quantitative stress analysis via statistical modelling was constructed to study the characteristic and formation of thermosonic Cu wire-Al bond pad system interfacial microstructure evolution. Objectives of this research are; (1) to study the characteristic and formation of Cu-Al IMC interfacial microstructure layer in thermosonic Cu wire-Al bond pad bonding process based on various bonding temperatures, Cu oxidation condition and HTS durations; (2) to study the influence of the Cu-Al IMC formation to the electrical contact resistance of the system. (3) to develop a theoretical model that describe the interfacial stress field of the Cu wire-Al bond pad system in terms of Cu-Al phase evolution. Microstructural characterizations were focused on Cu-Al IMC crystallographic system and compositional classification. Ball bond mechanical strength analysis were carried out to evaluate the bonding parameters with its strength. The bonding temperature was found to affect the thickness of the initial IMC layer formed at the bonding interface. The amount of the initial IMC formation in turn influences the saturation thickness of the IMC after HTS treatment. In the theoretical part, a stress model was proposed by coupling of both thermal misfit and diffusion induced stresses. It was found that the stress developed by interfacial Cu-Al IMC generally increased with the bonding temperature. The influence of forming gas supply was found to be less significant to affect the interfacial stress development, as the oxide layers did not hinder much the interdiffusion of Cu and Al atoms in the Cu-Al IMC formation. This report addressed the research gaps and presented a better understanding of the fundamental of interfacial Cu-Al IMC in thermosonic micro-interconnection. The results of the stress modelling could be a useful failure analysis technique for implementing Cu wire in the industry. In conclusion, the identified key parameters influencing Cu-Al IMC development and mechanical strength are in the following sequence: HTS duration > bonding temperature > forming gas supply as presented in the correlation matrix of various variables.

**SALING SAMBUNGAN MIKRO TERMOSONIK : KAJIAN PERTUMBUHAN
SEBATIAN ANTARA LOGAM ANTARA MUKA Cu-Al BERDASARKAN
PEMODELAN TEGASAN**

ABSTRAK

Salah satu teknologi ikatan dawai yang paling lazim yang melibatkan sambungan wayar logam kuprum, Cu ialah teknik ikatan termosonik. Namun, perubahan isipadu sebatian antara logam (SAL) yang terbentuk pada permukaan Cu dan tapak Al mendorong pembentukan ruang-ruang kosong dalam lapisan intermetalik Cu-Al. Ini amat ketara terutamanya selepas rawatan Penyimpanan Suhu Tinggi (PST). Kesan bebola udara bebas wayar Cu dan suhu sambungan dengan rawatan PST ke atas system intermetalik Cu-Al adalah tidak jelas disebabkan oleh pemerhatian yang berbeza-beza dan parameter sambungan wayar yang dikaji secara tidak konsisten. Pendekatan statistik dicadangkan adalah lebih berguna untuk menangani kekangan ini. Analisis tekanan kuantitatif melalui model statistik dipercayai boleh menutup jurang penyelidikan ini. Objektif penyelidikan ini adalah (1) untuk mengkaji ciri-ciri dan pembentukan struktur mikro antara ikatan dawai Cu pada permukaan pad Al, yang dijana melalui kaedah termosonik yang dimanipulasi berdasarkan pelbagai suhu ikatan, keadaan pengoksidaan Cu dan tempoh PST; (2) untuk mengkaji pengaruh pembentukan Cu-Al IMC kepada rintangan sentuhan dalam system elektrik unit tersebut; dan (3) untuk membangunkan model teori yang menerangkan medan tekanan antara muka sistem pad ikatan dawai-Al Cu dari segi evolusi fasa Cu-Al. Analisa mikrostruktur tertumpu pada sistem kristalografi intermetalik Cu-Al dan klasifikasi komposisi. Analisis kekuatan mekanikal ikatan bola dikaji untuk menyiasat kesan parameter ikatan dawai terhadap kekuatannya. Suhu ikatan didapati mempengaruhi ketebalan lapisan SAL awal yang terbentuk pada lapisan intermetalik Cu-Al. Kadar pembentukan SAL awal pula mempengaruhi ketebalan pembentukan SAL selepas rawatan PST. Dalam bahagian teori, model tekanan telah dicadangkan dengan gandingan kedua-dua ketidaksesuaian haba dan tekanan resapan dalam system intermetalik Cu-Al. Pemerhatian mendapati bahawa tekanan yang dibangunkan oleh lapisan SAL Cu-Al secara amnya meningkat dengan suhu proses ikatan dawai tersebut. Pengaruh pembentukan bekalan gas didapati kurang ketara dan tidak menjejaskan perkembangan tekanan antara muka yang jelas kerana lapisan oksida tidak banyak menghalang proses interdifusi antara atom-atom Cu dan Al dalam pembentukan lapisan SAL Cu-Al. Laporan ini menangani jurang penyelidikan dan membentangkan pemahaman yang lebih baik tentang asas pembentukan tekanan antara muka penyambungan Cu-Al termosonik. Keputusan pemodelan tegasan boleh menjadi suatu teknik analisis yang berguna untuk mengkaji penyambungan wayar Cu dalam industry secara lebih mendalam. Kesimpulannya, parameter utama yang dikenal pasti mempengaruhi perkembangan intermetalik Cu-Al adalah dalam tertib berikut: tempoh PST > suhu ikatan > bekalan gas pembentukan seperti yang dipersembahkan dalam matriks korelasi pelbagai pembolehubah.

ACKNOWLEDGEMENTS

First and foremost, I would like to express my utmost and unconditional gratitude to my supervisors, Professor Dr. T. Joseph Sahaya Anand and Professor Dr. Mohd Warikh bin Abd Rashid for their continuous support, confidence, patience, motivation and immense knowledge towards the completion of this research. I could not have imagined having better advisors and mentors for my studies.

I thank the dean, deputy deans, all the lecturers and staffs in the Faculty of Industrial and Manufacturing Technology and Engineering (previously known as Faculty of Manufacturing Engineering) and School of Graduate Studies, UTeM for their contributions in providing support and space for the successful completion of my studies. To my fellow colleagues, lab mates and technicians for the stimulating discussions and ideas on lab sessions, samples testing, sample analysis and for all the help they had offered.

Thank you to Dr. Lim Boon Huat, Dr. Chua Kok Yau and Mr. Lee Cher Chia from Infineon Technologies (Malaysia) Sdn Bhd. for the never-ending support and guidance throughout this journey. The guidance from your vast industry experience has helped me pull through.

To Collaborative Research in Engineering, Science and Technology (CREST), thank you for the platform, space and opportunity for a great collaborative research effort between UTeM and Infineon Technologies to create and grow Malaysian R&D ecosystem in the Electrical and Electronics economic sector.

I am as well most grateful to my family; father, mother and sisters whom have given me the support and courage throughout the course of this research as well as in my studies. My husband, Shashipal Singh, who pushed and pulled me through this, no words could thank you enough. To those involved directly or indirectly for their assistance in completing this research, thank you. To list out all of your names would be endless, so, thank you again. I offer my greatest wishes to all and may God bless all of you.

May 2024

TABLE OF CONTENTS

| | | Pages |
|------------------------------|--|----------|
| DECLARATION | | |
| APPROVAL | | |
| DEDICATION | | |
| ABSTRACT | | i |
| ABSTRAK | | ii |
| ACKNOWLEDGEMENTS | | iii |
| TABLE OF CONTENTS | | iv |
| LIST OF TABLES | | vii |
| LIST OF FIGURES | | viii |
| LIST OF APPENDICES | | xiii |
| LIST OF ABBREVIATIONS | | xiv |
| LIST OF SYMBOLS | | xvi |
| LIST OF PUBLICATIONS | | xviii |
| | | |
| CHAPTER | | |
| 1 | INTRODUCTION | 1 |
| | 1.1 Background | 1 |
| | 1.2 Problem Statement | 4 |
| | 1.3 Research Objectives | 4 |
| | 1.4 Scope | 5 |
| | 1.5 Chapter Outline | 5 |
| | 1.6 Significance of Studies | 7 |
| | | |
| 2 | LITERATURE REVIEW | 8 |
| | 2.1 Evolution of Wire Bonding Technology | 8 |
| | 2.2 Wire Bonding Techniques | 9 |
| | 2.2.1 Thermocompression Bonding | 9 |
| | 2.2.2 Ultrasonic Bonding | 10 |
| | 2.2.3 Thermosonic Bonding | 11 |
| | 2.2.4 Thermosonic Cu-Al Bonding Technology and Its Limitations | 13 |
| | 2.3 Forming Gas Supply | 14 |
| | 2.4 Wire Materials | 16 |
| | 2.5 Bond Pad Materials | 19 |
| | 2.6 Intermetallic Compounds (IMCs) Formation in Wire Bondings | 21 |
| | 2.7 Cu-Al Phase Diagram | 23 |
| | 2.7.1 Bonding Temperature and Its Effects on the Growth of Cu-Al Intermetallic Compound (IMC) Phases | 26 |

| | | |
|----------|---|-----------|
| 2.8 | Reliability Stress Tests | 27 |
| 2.9 | Characterization Techniques for Evaluating Cu-Al Bonding Interface | 29 |
| 2.9.1 | Ball Shear and Wire Pull Test | 31 |
| 2.9.2 | Field Emission Scanning Electron Microscope (FESEM) | 34 |
| 2.9.3 | Transmission Electron Microscope (TEM) | 35 |
| 2.9.4 | Energy Dispersive X-ray (EDX) | 38 |
| 2.10 | Stress Analysis | 38 |
| 2.11 | Summary | 41 |
| 3 | METHODOLOGY | 44 |
| 3.1 | Introduction | 44 |
| 3.2 | The Synthesis of Cu Wire-Al Bond Pad Samples | 46 |
| 3.2.1 | Design of Experiment | 48 |
| 3.3 | Sample Preparation for Characterization | 50 |
| 3.3.1 | Mechanical Cross-Section for Microscopic Analysis | 50 |
| 3.3.2 | Focused Ion Beam (FIB) Milling for Lamella Extraction | 51 |
| 3.3.3 | Encapsulation of Wire Bond for Electrical Studies | 52 |
| 3.4 | Characterizations of Cu-Al Samples | 53 |
| 3.5 | Modelling of Stress Developed at Cu-Al Bonding Interface | 56 |
| 3.5.1 | Equations for Thermal Misfit and Diffusion-Induced Stresses | 56 |
| 3.5.2 | Predictions of Material Properties of Solid Solution | 61 |
| 3.5.3 | Relationship between Concentrations (C_s , C_i and x) | 63 |
| 3.5.4 | Partial Molar Volume of Solid Solution | 64 |
| 3.6 | Summary | 67 |
| 4 | RESULTS AND DISCUSSIONS | 68 |
| 4.1 | Ball Shear Test (BST) | 69 |
| 4.2 | Wire Pull Test (WPT) | 71 |
| 4.3 | Electron Microscopy Analysis | 73 |
| 4.3.1 | Cu-Al Samples Synthesized at 150°C | 74 |
| 4.3.1.1 | FESEM-EDX Analysis for Samples Synthesized at 150°C, Forming Gas ON | 74 |
| 4.3.1.2 | TEM-EDX Analysis for Samples Synthesized at 150°C | 80 |
| 4.3.2 | Cu-Al Samples Synthesized at 280°C | 85 |
| 4.3.2.1 | FESEM-EDX Analysis for Samples Synthesized at 280°C, Forming Gas ON | 85 |
| 4.3.2.2 | TEM-EDX Analysis for Samples Synthesized at 280°C | 90 |
| 4.3.3 | Cu-Al Samples Synthesized at 400°C | 95 |
| 4.3.3.1 | FESEM-EDX Analysis for Samples Synthesized at 400°C, Forming Gas ON | 95 |
| 4.3.3.2 | TEM-EDX Analysis for Samples Synthesized at 400°C | 101 |
| 4.4 | Current–Voltage (I–V) Analysis for Samples Synthesized at 280°C, Forming Gas ON | 108 |

| | | |
|----------|---|------------|
| 4.5 | Correlation Studies between HTS Durations, IMC Thickness, Mechanical Bond Strength and Electrical Studies | 109 |
| 4.6 | Relationship between Ball Shear Strength and Bonding Parameters | 111 |
| 4.7 | Grain Boundary Diffusion at Low Bonding Temperature | 113 |
| 4.8 | The Presence of Oxide Layers at the Bonding Interface | 114 |
| 4.9 | Formation of Gaps and Voids Within the IMC Layers | 114 |
| 4.10 | Theoretical Modelling | 115 |
| | 4.10.1 Prediction of Elastic Properties of Solid Solution | 115 |
| | 4.10.2 Prediction of Concentration of Solute and Partial Molar Volume of Solid Solution | 119 |
| | 4.10.3 Prediction of Stresses | 121 |
| | 4.10.4 Stress Analysis to Evaluate the Effect of Bonding Temperatures | 122 |
| | 4.10.5 Stress Analysis to Assess the Effect of HTS Treatment | 125 |
| | 4.10.6 Stress Analysis to Evaluate the Effect of Forming Gas Supply | 127 |
| 4.11 | Summary | 129 |
| 5 | CONCLUSION AND RECOMMENDATIONS | 131 |
| 5.1 | Conclusion | 131 |
| 5.2 | Recommendation for Future Studies | 133 |
| | REFERENCES | 134 |
| | APPENDICES | 150 |

LIST OF TABLES

| Table | Title | Pages |
|--------------|--|--------------|
| 2.1 | Comparison between wire bonding technologies | 13 |
| 2.2 | Industrially optimized thermosonic wire bonding parameters used to synthesize Cu-Al samples | 14 |
| 2.3 | Micro-structural and physical properties of Cu-Al phases | 25 |
| 2.4 | Cu-Al phase formation after HTS under thermosonic wire bonding | 27 |
| 2.5 | Description of failure codes in ball shear test | 32 |
| 2.6 | Description of failure codes in wire pull test | 33 |
| 3.1 | Optimized parameters used to synthesize samples | 48 |
| 3.2 | Full factorial sample matrix of Cu-Al samples | 49 |
| 4.1 | Mean (\bar{x}) and standard deviation (σ) values of ball shear strength measurement | 69 |
| 4.2 | Mean (\bar{x}) and standard deviation (σ) values of wire pull strength measurement | 71 |
| 4.3 | Summary of EDX analysis of sample synthesized at 150°C | 79 |
| 4.4 | Summary table for the Cu-Al phase identification for samples R1-R6 | 84 |
| 4.5 | Summary of EDX analysis of sample synthesized at 280°C | 90 |
| 4.6 | Summary table for the Cu-Al phase identification for samples R7-R12 | 94 |
| 4.7 | Summary of EDX analysis of sample synthesized at 400°C | 100 |
| 4.8 | Summary table for the Cu-Al phase identification for samples R13-R18 | 104 |
| 4.9 | Summary of the thickness of the Cu-Al IMC and Cu-Al phase identification with the individual wire bonding parameters | 106 |
| 4.10 | Summary of the resistivity values of the samples | 109 |
| 4.11 | Material related constants used in the analysis | 116 |

LIST OF FIGURES

| Figure | Title | Pages |
|---------------|---|--------------|
| 2.1 | Thermocompression wire bonding process (Integrated Circuit Engineering Corporation, 1997) | 9 |
| 2.2 | Ultrasonic wire bonding process (Integrated Circuit Engineering Corporation, 1997) | 11 |
| 2.3 | Thermosonic wire bonding process (Integrated Circuit Engineering Corporation, 1997) | 12 |
| 2.4 | Schematic diagram of the forming gas supply tool in a wire bonder (Hang et. al., 2005) | 15 |
| 2.5 | An ideal shape (left) and distorted (right) Cu FAB formation | 16 |
| 2.6 | Cross section of a Cu wire to Al bond pad and its Cu-Al IMC phases (Appelt, 2012) | 22 |
| 2.7 | The Cu-Al phase diagram (Pelzer et. al., 2014) | 24 |
| 2.8 | Cu-Al crystal structures with increasing Al content (Wei et. al., 2009) | 25 |
| 2.9 | Schematic diagram of ball bond lift failure mode in ball shear test | 31 |
| 2.10 | Schematic diagram of wire pull test | 33 |
| 2.11 | Schematic illustration of different components in a TEM microscope (Minh, 2019) | 37 |
| 3.1 | Flow chart of the thermosonic micro-interconnections and interfacial IMC growth formation study | 45 |
| 3.2 | The illustration of the structure of the synthesized thermosonic Cu-Al sample in its un-encapsulated form | 46 |
| 3.3 | Actual X-ray photo of an encapsulated unit used in this research | 46 |
| 3.4 | The lifting of the lamella piece taken from the central region of the bonding interface | 52 |

| | | |
|------|--|----|
| 3.5 | Schematic diagram of a cross section of a simple encapsulated device | 53 |
| 3.6 | Photo of the encapsulated unit used for I-V analysis | 53 |
| 3.7 | Circuit diagram for I-V analysis | 55 |
| 3.8 | The geometrical considerations of the multi-layer structure | 59 |
| 3.9 | The illustration of the process flow of the stress calculation. (a) The composition measurements, (b) the calculated xCu profile from (a), (c) the converted C profile, (d) Predicted elastic material properties, (e) predicted stresses profile | 66 |
| 4.1 | OM images of (a) symmetrical non-oxidized ball bond and (b) asymmetrical and off-centred oxidized ball bond (Chua et al., 2012) | 68 |
| 4.2 | Smearing of Cu ball bond on Al bond pad after ball shear test | 69 |
| 4.3 | Comparison of mean ball shear strength on all samples | 70 |
| 4.4 | Sample showing broken wire after wire pull test | 72 |
| 4.5 | Comparison of mean wire pull strength on all samples | 73 |
| 4.6 | A quality polished cross section of a Cu ball bond on Al bond pad (Magnification 100X) | 74 |
| 4.7 | FESEM images of the cross-sectioned sample (R1) wire bonded at 150°C, forming gas ON, without heat treatment | 76 |
| 4.8 | FESEM images of the cross-sectioned sample (R2) wire bonded at 150°C, forming gas ON, after 500 hours HTS | 77 |
| 4.9 | FESEM images of the cross-sectioned sample (R3) wire bonded at 150°C, forming gas ON, after 1000 hours HTS | 78 |
| 4.10 | TEM and EDX line scan composition profile for sample (R1) wire bonded at 150°C, forming gas ON, without heat treatment. | 80 |
| 4.11 | TEM and EDX line scan composition profile for sample (R2) wire bonded at 150°C, forming gas ON, after 500 hours HTS | 81 |
| 4.12 | TEM and EDX line scan composition profile for sample (R3) wire bonded at 150°C, forming gas ON, after 1000 hours HTS | 81 |
| 4.13 | TEM and EDX line scan composition profile for sample (R4) wire bonded at 150°C, forming gas OFF, without heat treatment | 82 |

| | | |
|------|--|----|
| 4.14 | TEM and EDX line scan composition profile for sample (R5) wire bonded at 150°C, forming gas OFF, after 500 hours HTS | 82 |
| 4.15 | TEM and EDX line scan composition profile for sample (R6) wire bonded at 150°C, forming gas OFF, after 1000 hours HTS | 83 |
| 4.16 | Graph of total IMC thickness versus HTS duration for samples R1-R6 | 84 |
| 4.17 | FESEM images of the cross-sectioned sample (R7) wire bonded at 280°C, forming gas ON, without heat treatment | 86 |
| 4.18 | FESEM images of the cross-sectioned sample (R8) wire bonded at 280°C, forming gas ON, after 500 hours HTS | 87 |
| 4.19 | FESEM images of the cross-sectioned sample (R9) wire bonded at 280°C, forming gas ON, after 1000 hours HTS | 89 |
| 4.20 | TEM and EDX line scan composition profile for sample (R7) wire bonded at 280°C, forming gas ON, without heat treatment | 91 |
| 4.21 | TEM and EDX line scan composition profile for sample (R8) wire bonded at 280°C, forming gas ON, after 500 hours HTS | 91 |
| 4.22 | TEM and EDX line scan composition profile for sample (R9) wire bonded at 280°C, forming gas ON, after 1000 hours HTS | 92 |
| 4.23 | TEM and EDX line scan composition profile for sample (R10) wire bonded at 280°C, forming gas OFF, without heat treatment | 92 |
| 4.24 | TEM and EDX line scan composition profile for sample (R11) wire bonded at 280°C, forming gas OFF, after 500 hours HTS | 93 |
| 4.25 | TEM and EDX line scan composition profile for sample (R12) wire bonded at 280°C, forming gas OFF, after 1000 hours HTS | 93 |
| 4.26 | Graph of total IMC thickness versus HTS duration for samples R7-R12 | 95 |
| 4.27 | FESEM images of the cross-sectioned sample (R13) wire bonded at 400°C, forming gas ON, without heat treatment | 96 |
| 4.28 | FESEM images of the cross-sectioned sample (R14) wire bonded at 400°C, forming gas ON, after 500 hours HTS | 98 |
| 4.29 | FESEM images of the cross-sectioned sample (R15) wire bonded at 400°C, forming gas ON, after 1000 hours HTS | 99 |

| | | |
|------|---|-----|
| 4.30 | TEM and EDX line scan composition profile for sample (R13) wire bonded at 400°C, forming gas ON, without heat treatment | 101 |
| 4.31 | TEM and EDX line scan composition profile for sample (R14) wire bonded at 400°C, forming gas ON, after 500 hours HTS | 101 |
| 4.32 | TEM and EDX line scan composition profile for sample (R15) wire bonded at 400°C, forming gas ON, after 1000 hours HTS | 102 |
| 4.33 | TEM and EDX line scan composition profile for sample (R16) wire bonded at 400°C, forming gas OFF, without heat treatment | 102 |
| 4.34 | TEM and EDX line scan composition profile for sample (R17) wire bonded at 400°C, forming gas OFF, after 500 hours HTS | 103 |
| 4.35 | TEM and EDX line scan composition profile for sample (R18) wire bonded at 400°C, forming gas OFF, after 1000 hours HTS | 103 |
| 4.36 | Graph of total IMC thickness versus HTS duration for samples R13-R18 | 105 |
| 4.37 | Box plot of the resistivity values of the samples | 108 |
| 4.38 | Correlation matrix of various variables in the test | 110 |
| 4.39 | Correlation between IMC thickness with mechanical strength of wires bonded with forming gas ON | 112 |
| 4.40 | (a) The reference model of Cu-Al metal couple with a layer of solid solution sandwiched between the pure metals. (b) The plot of Cu concentration versus the thickness of the solid solution. | 116 |
| 4.41 | The comparison of reported and predicted values of (a) shear, (b) bulk and (c) Young's moduli | 118 |
| 4.42 | The plot of the predicted solute concentration, C versus fractional concentration of Cu, x_{Cu} | 120 |
| 4.43 | The plot of the calculated partial molar volume of the solid solution, \tilde{V} versus x_{Cu} | 120 |
| 4.44 | The calculated distribution of three components of the diffusion induced stress | 121 |

- 4.45 (a) TEM images on the IMC formation at the bonding interface.
 (b) The corresponding Cu concentration distribution. (c) The corresponding predicted stresses. (i) to (iii) represent the results of the samples synthesized at 150, 280 and 400°C with FG ON, HTS 1000hrs 124
- 4.46 (a) TEM images on the IMC formation at the bonding interface.
 (b) The corresponding Cu concentration distribution. (c) The corresponding predicted stresses. (i) to (iii) represent the results of the samples treated at HTS 0, 500 and 1000 hours; synthesized at 280°C with FG ON 126
- 4.47 (a) TEM images on the IMC formation at the bonding interface.
 (b) The corresponding Cu concentration distribution. (c) The corresponding predicted stresses. (i) to (ii) represent the results of the samples synthesized with forming gas ON and OFF, synthesized at 400°C treated with HTS 500hrs 128



LIST OF APPENDICES

| Appendix | Title | Pages |
|----------|--|-------|
| A | Derivations of ε_{t0} , ρ_t , ε_{c0} And ρ_c | 150 |
| B | Derivations of Conversion Equations | 155 |
| C | Derivation of The Number of Mole of Solute Atoms Per Unit Volume, C | 158 |



LIST OF ABBREVIATIONS

| | |
|-------|---|
| Al | - Aluminum |
| Au | - Aurum |
| BSE | - Back Scattered Electron |
| BST | - Ball Shear Test |
| CTE | - Coefficient of Thermal Expansion |
| Cu | - Copper |
| EDX | - Energy Dispersive X-Ray |
| EFO | - Electronic Flame Off |
| FAB | - Free Air Ball |
| FCC | - Face Centered Cubic |
| FESEM | - Field Emission Scanning Electron Microscope |
| FG | - Forming Gas |
| HTS | - High Temperature Storage |
| IMC | - Intermetallic Compound |
| IC | - Integrated Circuit |
| JEDEC | - Joint Electron Device Engineering Council |
| SEM | - Scanning Electron Microscope |
| Pd | - Palladium |
| SiC | - Silicon Carbide |
| Si | - Silicon |
| HAADF | - High Angle Annular Dark Field |
| TEM | - Transmission Electron Microscope |

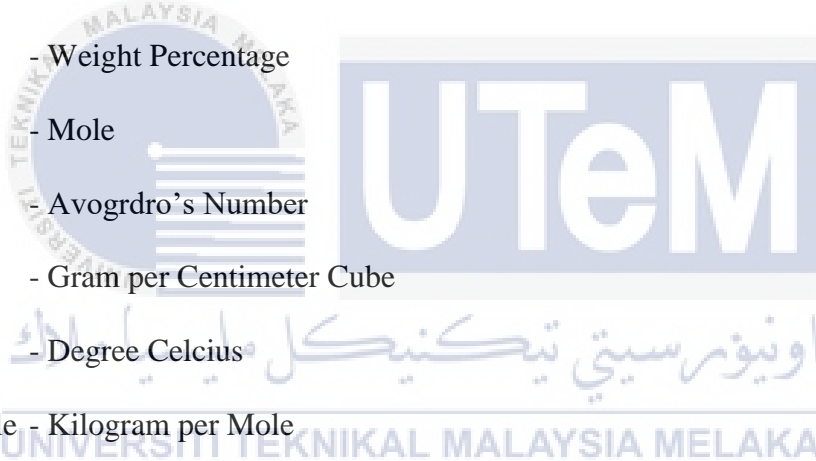
- WPT - Wire Pull Test
- TC - Temperature Cycling
- PCT - Pressure Cooker Test
- OM - Optical Microscope
- XRD - X-Ray Diffraction



LIST OF SYMBOLS

| | |
|---------------|---|
| ρ | - Radius Of Curvature |
| μ | - Shear Modulus |
| σ | - Stress |
| E | - Elastic Modulus |
| κ | - Bulk Modulus |
| α | - Coefficient of Thermal Expansion |
| T | - Temperature |
| s | - Substrate |
| i | - Layer-i |
| ε | - Normal Strain At x-axis |
| D | - Mass Density |
| \bar{V} | - Partial Molar Volume |
| A | - Atomic Weight |
| ΔV | - Volume Change |
| V | - Volume |
| R | - Atomic Radius |
| n | - Number of Mole |
| α -Al | - Al Phase |
| θ | - CuAl ₂ Phase |
| η 2 | - CuAl Phase |
| ξ 2 | - Cu ₄ Al ₃ Phase |
| δ | - Cu ₃ Al ₂ Phase |

| | |
|---------------------|---|
| γ_1 | - Cu ₉ Al ₄ Phase |
| α_2 | - Cu Phase |
| (Cu) | - Cu Rich Terminal Solid Solution |
| (Al) | - Al Rich Terminal Solid Solution |
| A | - Area |
| C | - Concentration of Solute |
| GPa | - Giga Pascal |
| Å | - Armstrong |
| nm | - nanometer |
| at% | - Atomic Percentage |
| wt% | - Weight Percentage |
| mole | - Mole |
| NA | - Avogadro's Number |
| gcm ⁻³ | - Gram per Centimeter Cube |
| °C | - Degree Celcius |
| kg/mole | - Kilogram per Mole |
| kg/m ³ | - Kilogram per Meter Cube |
| mole/m ³ | - Mole per Meter Cube |
| µm | - Micrometer |
| \bar{x} | - Mean Value |
| σ | - Standard Deviation Value |



LIST OF PUBLICATIONS

Journals

Parts of this thesis have been published in:

Chua Kok Yau, T. Joseph Sahaya Anand, **S. Shariza**, Yong Foo Khong, Lee Cher Chia, Lim Boon Huat, Ranjit Singh and R.T. Rajendra Kumar, 2020. Statistical analysis on the mechanical and micro-structural characteristics of thermosonic Cu-Al interconnection. *Microelectronics Reliability*, 109, pp. 113664.

S. Shariza, T. Joseph Sahaya Anand, Chua Kok Yau, Lim Boon Huat and Lee Cher Chia, 2019. Evaluation of bond shear strength of heat treated Cu-Al bonding interface. *International Journal of Innovative Technology and Exploring Engineering*, 8(7S), pp. 346-353.

S. Shariza, T. Joseph Sahaya Anand, A.R.M. Warikh, Lee Cher Chia, Chua Kok Yau and Lim Boon Huat, 2018. Bond strength evaluation of heat treated Cu-Al wire bonding. *Journal of Mechanical Engineering and Sciences*, 12(4), pp. 4275-4284.

T. J. S. Anand, K.Y. Chua, **S. Shariza**, C.C. Lee and D. Ranjith Kumar, 2018. Effects of the bonding temperature and annealing towards the micro-structural of thermosonic Cu-Al interface. *International Journal of Scientific & Engineering Research*, 9(12), pp. 264-286.

Lee Cher Chia, Chua Kok Yau, T. Joseph Sahaya Anand, **S. Shariza** and Mohamad Ridzuan Bin Jamli, 2017. Modelling of wire bonding Cu-Al intermetallic formation growth towards interfacial stress, *19th Electronics Packaging Technology Conference Proceedings, IEEE*, pp. 1-5.

Conferences

Parts of this thesis have been presented in:

T. Joseph Sahaya Anand, **S. Shariza**, Chua Kok Yau, A.R.M. Warikh, Kok-Tee Lau and Lim Boon Huat. Electrical studies of Cu wire interconnections in electronic packages upon high temperature storage. Presented at: *The 4th International Symposium in Research in Innovation and Sustainability (ISoRIS 2019)*, 28-29 August 2019, Penang, Malaysia.

Won the Best Paper Award.

S. Shariza, T. Joseph Sahaya Anand, Lee Cher Chia, Chua Kok Yau and Lim Boon Huat. Bond shear strength evaluation of heat treated Cu-Al bonding interface. Presented at: *The 1st International Conference of Electrical, Electronic & Optical Engineering (ICEEOE 2018)*, 10-11 November 2018, Seremban, Malaysia.

Won the Best Paper Award.

